Gas puff imaging of edge turbulence (invited)

R. J. Maqueda and G. A. Wurden
Los Alamos National Laboratory, Los Alamos, New Mexico 87545

D. P. Stotler and S. J. Zweben
Princeton Plasma Physics Laboratory, Princeton, New Jersey 08540

B. LaBombard and J. L. Terry
MIT Plasma Science and Fusion Center, Cambridge, Massachusetts 02139

J. L. Lowrance, V. J. Mastrocola, and G. F. Renda
Princeton Scientific Instruments, Monmouth Junction, New Jersey 08852

D. A. D'Ippolito and J. R. Myra
Lodestar Research Corporation, Boulder, Colorado 80301

N. Nishino
Hiroshima University, Hiroshima, Japan

(Presented on 10 July 2002)

The gas puff imaging (GPI) diagnostic can be used to study the turbulence present at the edge of magnetically confined plasmas. In this diagnostic the instantaneous two-dimensional (2D) radial vs poloidal structure of the turbulence is measured using fast-gated cameras and discrete fast chords. By imaging a controlled neutral gas puff, of typically helium or deuterium, the brightness and contrast of the turbulent emission fluctuations are increased and the structure can be measured independently of natural gas recycling. In addition, recent advances in ultrafast framing cameras allow the turbulence to be followed in time. The gas puff itself does not perturb the edge turbulence and the neutral gas does not introduce fluctuations in the emission that could possibly arise from a nonsmooth (turbulent) neutral gas puff. Results from neutral transport and atomic physics simulations using the DEGAS 2 code are discussed showing that the observed line emission is sensitive to modulations in both the electron density and the electron temperature. The GPI diagnostic implementation in the National Spherical Torus Experiment (NSTX) and Alcator C-Mod tokamak is presented together with example results from these two experiments. [DOI: 10.1063/1.1535249]

I. INTRODUCTION

Plasma turbulence at the edge of magnetically confined plasmas has been previously observed as broadband fluctuations in visible light emission,[1,2] as well as measured with Langmuir probes[3,4] and beam emission spectroscopy (BES).[5] The transport at the edge and across the scrape-off layer depends on the level and characteristics of this turbulence and, consequently, so do the edge temperature and density. The edge conditions then may affect the core confinement through their effect on edge gradients and gradient driven instabilities such as drift waves. Possibly, also, the edge turbulence may play an important role in high confinement physics (i.e., H-mode physics) where steep edge pedestals in the temperature and density form within the closed field line region in proximity to the separatrix. The ubiquitous edge turbulence, seen in TFTR,[6,7] Asdex,[3] Alcator C-Mod,[1,8] DIII-D,[5] NSTX,[2] and other devices[4,9,10] is also conjectured to be related to density limit observed with very similar scaling in devices as diverse as large aspect ratio tokamaks, spherical tori, and reversed field pinches. In this paper we present a new diagnostic, termed gas puff imaging (GPI), that can be employed to study edge turbulence.

The visible emission from the edge of toroidally confined plasmas is modulated, in principle, by both the local temperature and density fluctuations. This visible emission from neutral atoms recycled from the vessel walls, is also dependent on the amount of recycling. In the GPI diagnostic, a controlled neutral gas puff, of typically helium or deuterium, is injected at the edge of the torus and the visible light emission from the gas cloud (HeI line at 587.6 nm or D_α line at 656.2 nm) is then imaged with short exposures, shorter than the autocorrelation time of the turbulence. The images obtained, typically in the radial vs poloidal plane, correspond then directly to the instantaneous structure of the turbulence, without the need to infer this structure from statistical correlations between a small number of measurements such as those of Langmuir probes. In addition, if the framing rate of the camera employed is faster than the lifetime of the turbulent structures within the field of view, the motion of the turbulence can be followed. Recent advances in CCD detector technology allows the turbulence to be followed in this manner without the need for mechanical framing cameras or chemical emulsion films.

GPI diagnostics have been implemented in both the National Spherical Torus Experiment (NSTX) (Ref. 11) and the high aspect ratio Alcator C-Mod tokamak.[12] The setup in

both of these toroidal devices is presented in Sec. II together with some discussion on diagnostics issues such as resolution and image interpretation, which are closely related to the atomic physics for the gas being puffed. Some results from NSTX and Alcator C-mod are given in Sec. III. The article concludes with a summary and discussion of the advantages and difficulties of the GPI diagnostics, relative to other diagnostics employed in the study of edge turbulence.

II. THE GAS PUFF IMAGING DIAGNOSTIC

In the GPI diagnostic a neutral gas, typically helium or deuterium, is puffed at the edge of the torus and the visible line emission from the gas cloud, for example, the HeI line at 587.6 nm or D_α at 656.2 nm, is imaged by means of fast-framing cameras and linear detector arrays. These measurements are performed with high spatial resolution and employing individual frame exposures (time resolution for the case of the detector arrays) shorter than the autocorrelation time of the turbulent structures. This emission, under the collisional radiative approximation, and assuming negligible time-dependent effects, will depend on the local electron density n_e and temperature T_e as

$$S(\text{photons/s m}^3) = n_o f(n_e, T_e) A, \tag{1}$$

where n_o is the local neutral density, A is the radiative decay rate for the observed line, and $f(n_e, T_e)$ is a function that gives the density ratio between neutrals in the upper state of the transition to those in the ground state. The decay rate A being much larger than the inverse of the autocorrelation time of the fluctuations (which is typically greater than 10 μs), ensures that the emission observed corresponds to the local plasma parameters. The dependence on n_e and T_e, through the function f, modulates the line emission according to the fluctuations in both these two plasma parameters. The actual dependence, obtained from modeling the collisional and radiative processes affecting the individual excited states of the neutral gas, will be discussed in Sec. II B.

Of particular importance for the success of GPI as a diagnostic for edge turbulence are the assumptions that the gas puff does not perturb the edge turbulence significantly and that the neutral gas does not introduce fluctuations through the neutral density, n_o in Eq. (1). Both of these assumptions will be justified later on in this section.

It has been observed, and reported elsewhere,[2,13] that the turbulence correlation length along the magnetic field lines is much longer that the correlation length in the transverse directions, i.e., radial and poloidal directions. Consequently, the most interesting plane to observe the turbulence is on this radial vs poloidal plane, that is, observe the gas puff emission with a line of sight parallel to the local magnetic field at the gas cloud. We briefly describe below the hardware implemented in the National Spherical Torus Experiment (NSTX) and the Alcator C-Mod tokamak that allows GPI measurements to be performed in these two devices.

A. Diagnostic setup

A gas puff imaging diagnostic has been developed for NSTX, a low aspect ratio tokamak (minor radius $a = 67$ cm and major radius $R = 85$ cm) that operates at toroidal magnetic fields typically in the 0.3–0.45 T range. The in-vessel diagnostic setup in NSTX can be seen in Fig. 1(a). The gas is injected through a 29 cm long pipe with 30 equally spaced, 1 mm diam holes on its plasma facing side. The elongated emitting gas cloud, that is then located just above the midplane on the low field side of the torus, is imaged through a re-entrant window placed so that the gas cloud is observed along a field line when the experiment is run at 0.9 MA of toroidal plasma current and 0.35 T of toroidal field, a ~42° angle respect to horizontal. The window is shuttered off during glow discharge cleaning and boronization to avoid coatings being deposited on its surface. A 30 cm×30 cm (approx.) viewing area at the gas cloud plane is imaged into a

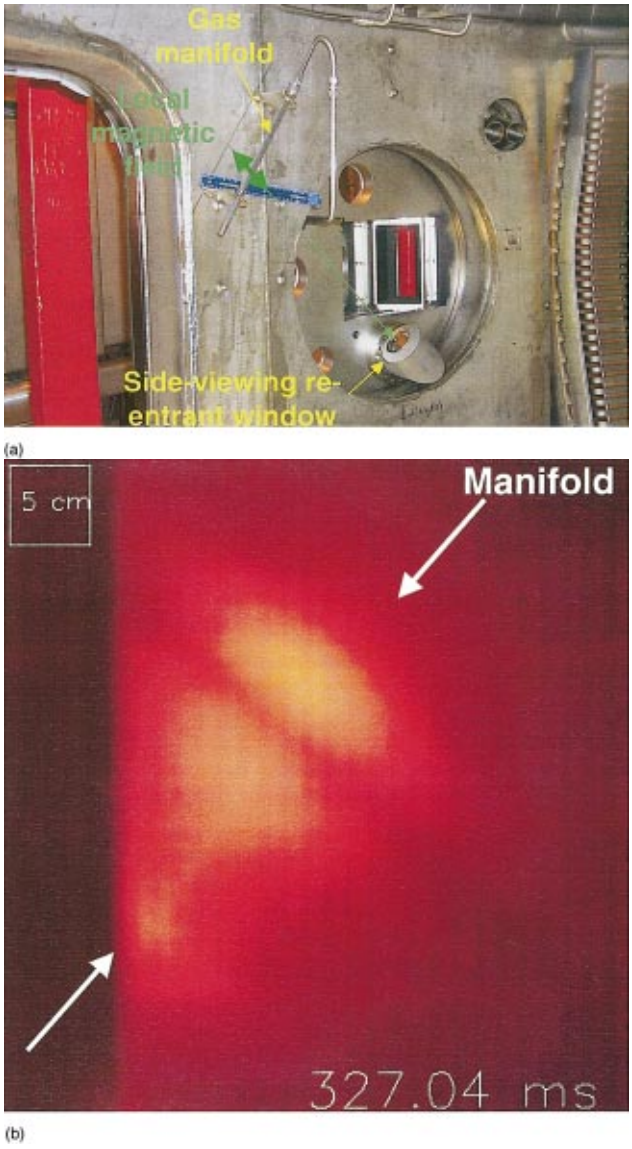

FIG. 1. (Color) Gas puff imaging diagnostic setup in NSTX. The in-vessel components of the setup, including the re-entrant viewing port and the linear gas manifold can be seen in (a). The emission from the elongated gas cloud produced by the manifold is imaged along the direction of the local magnetic field line. (b) shows an image of the gas cloud, obtained with a 74 μs exposure and a HeI interference filter (587.6 nm), as observed from a window on the opposite site of the vessel (shot 108975). The structure seen on the neutral line emission follows the local field line.

TABLE I. Imaging cameras used in NSTX and Alcator C-Mod.

	Xybion (analog)	Kodak EM1012	Phantom v.4	PSI-3[a]	PSI-4[a]
Intensified	Yes	Yes	Yes (ILS-3)	No	No
Array size (pixels)	640×240	239×192	512×512	64×64	160×80
Frame speed (frames/s)	60	1000	1000	⩽5 000 000	⩽1 000 000
Max. speed (frames/s)	…	6000	32000	…	…
Frame storage	(video)	1638	4000	12	28
Usage	C-Mod	NSTX	NSTX	C-Mod	NSTX

[a]Princeton Scientific Instruments.

400 pixel×400 pixel coherent fiber optic bundle. The other end of this bundle is then imaged either into fast-gated cameras or a linear array of 7 photomultiplier tubes with the use of a beamsplitter. Each of these 7 tubes is used then to record the emission from an ~2 cm diam area of the gas cloud along a radial chord of the plasma with ~100 kHz bandwidth. (This array of 7 tubes was later upgraded to 13 tubes in a radial-poloidal cross pattern.) Helium, deuterium, and argon have been puffed in NSTX, although only results in He will be shown in this article. An interference filter centered at 587.6 nm is used to select the $3\,^3D-2\,^3P$ HeI line transition at this wavelength. Typically, a helium influx of $\sim 6\times 10^{20}$ atoms/s is injected for about ~50 ms. Figure 1(b) show an image of the He gas cloud as observed from a window located ~180° toroidally, opposite to the gas manifold. The shadow of the 20 cm radius center column of NSTX can be seen on the left side of this image. The re-entrant window used for GPI is located towards the bottom right of this image, although not in its field of view. The structure of the HeI emission seen in this figure is oriented along the magnetic field direction at the gas cloud location and the time-averaged emission is ~24 cm wide (FWHM) along this direction.

The GPI system in Alcator C-Mod is in many ways similar to that in NSTX. (A schematic view of the in-vessel hardware can be seen in Fig. 1 of Ref. 8.) The gas is puffed radially into the edge of the plasma through a single-point 3 mm diam nozzle rather than an elongated, multihole manifold. The gas cloud is viewed with an in-vessel telescope aimed at the puff from a direction along the local magnetic filed line (~11° respect to horizontal). An area of approximately 6 cm×6 cm just below the midplane is imaged, through a small window, onto the 400 pixel×400 pixel coherent fiber optic bundle. The fast-gated camera then images the other end of this bundle. A separate in-vessel telescope and three discrete optical fibers are used to capture, using fast photodiodes and high-gain broadband amplifiers, the time evolution of the emission in 3.5 mm diam spots located radially along the gas cloud. Both deuterium and helium have been used as puffed gases in Alcator C-Mod. Nevertheless, only results with D_2 will be presented in this paper and, in this case, interference filters for the D_α line (656.2 nm) are used in both the imaging camera and discrete viewing chords. Typically $10^{19}-10^{20}$ atoms/s are puffed steadily during the current flat-top of the plasma discharge. The gas cloud produced in this manner has, in the vicinity of the separatrix, a ~6 cm (FWHM) extension along the field line direction.

Several different imaging cameras have been used in NSTX and Alcator C-Mod to capture the instantaneous 2D radial vs poloidal, structure of the neutral gas emission. The main characteristics of these cameras can be seen in Table I. While the framing speed of these cameras range from 60 frames/s in the case of the intensified Xybion video camera to 1 000 000 frame/s in the devices from Princeton Scientific Instruments, a common ability of these cameras is that the exposure of each frame can be reduced to 10 μs or shorter and in this way ''freeze'' the turbulence.

The ultrafast PSI-3 and PSI-4 cameras allow the turbulence to be followed in time producing ''moving'' image sequences and not just uncorrelated snapshots like those obtained at much smaller framing speeds. The special CCD in the PSI cameras has the facility of storing the images within the sensor itself, thus circumventing the bandwidth problems normally associated with digitizing the array and storing the data in memory banks common to high frame-rate digital cameras such as the Kodak EM1012 and Phantom v.4. Each pixel of the PSI cameras consists of a photodetector and a CCD-type charge-storage memory array. In each clock cycle of the camera, photoelectrons generated by the photodetector are shifted into the adjacent charge storage sites of the pixel's memory array, thereby acquiring a frame. Once the acquisition is completed, the charge in the storage sites is digitized at a slower rate. Although the PSI cameras are not intensified, their net quantum efficiency of ~30% at the wavelengths of interest allow short exposures ($\leqslant 10$ μs) to be used.

B. Diagnostic issues

The spatial resolution of the optical system is 2–3 mm at the gas puff plane in both NSTX and Alcator C-Mod. Nevertheless, as the emitting cloud extends toroidally, and with it the embedded turbulent structure, due to the curvature of the flux surfaces in the plasma the observed structures will potentially extend radially degrading the radial resolution. In a similar way if the line of sight is not parallel to the local magnetic field line direction, there can be loss of poloidal

resolution when observing the turbulent structures which lies along this field line. Both of these loss-of-resolution effects are bigger the larger the neutral gas cloud is in the direction line of sight direction. In the case of NSTX the gas puff manifold is 15–20 cm from the plasma edge and consequently, as seen in connection with Fig. 1(b) the gas cloud extends ~24 cm along the line of sight (which is close to the field line direction). As a result the radial resolution degrades to ⩽3 cm radially. On the other hand, if the plasma current and toroidal field are selected so that the pitch angle at the gas cloud is close to the ~42° from which the gas cloud is observed the poloidal resolution remains close to the 3 mm dictated by the optical system. In Alcator C-Mod, the gas puff nozzle is much closer to the plasma edge (~2.5 cm) and hence the gas cloud extends only ~6 cm along the line of sight. This extent is not large enough to produce any substantial degradation in the radial and poloidal resolutions, as long as the pitch angle at the gas cloud remains close to the 11° respect to horizontal for which the hardware is optimized.[8]

A key assumption for the success of GPI as a diagnostic for edge turbulence is that neutral gas does not introduce fluctuations through the neutral density n_o or, in other words, that the neutral density is smooth within the gas cloud. By looking at images such as that in Fig. 1(b) and similar ones obtained with exposures a factor 3 shorter, one can see that this assumption is justified. The structure observed in the emission in these images is aligned with the magnetic field and corresponds to fluctuations in the electron density and temperature. No structure is seen along the field line direction where fluctuations due to the neutral density should be discernable. Along the field line direction only an emission distribution resembling a Gaussian has been observed corresponding to the gas flow pattern from the nozzle or the openings in the linear manifold. A similar result was obtained in experiments that characterized neutral gas flow from nozzles into vacuum for laser-gas interaction research.[14] In these experiments too very smooth spatial distributions in the neutral gas density were inferred. The basic physics behind these smooth distributions may be that the neutral gas flow becomes collisionless just past the nozzle or openings and hence any density gradients or structure that the neutral density may have at the nozzle tip is smoothed out by the random velocity distribution by the time the atoms get to the plasma edge.

Also key to the success of GPI as a diagnostic for edge turbulence is the assumption that the neutral gas puff does not affect nor produce fluctuations. One possible mechanism for this may be due to increased energy losses due to ionization and/or radiation. Nevertheless there is ample empirical evidence that the gas puff does NOT affect the edge turbulence being diagnosed. In first place, it was observed in Alcator C-Mod that the frequency spectrum of the D_α fluctuations as measured by the fast diodes is similar to the spectrum of fluctuations in the ion saturation current measured by a Langmuir probe at the same radius (see, for instance, Fig. 5 of Ref. 8). Second, the spatial structure, frequency spectrum, and relative fluctuation levels of the gas cloud emission did not vary significantly when the gas flow rate was varied over the 10^{19}–10^{20} atoms/s range in Alcator C-Mod and over a factor 5 in NSTX. An example of this lack of perturbation can be seen in Fig. 2, where the frequency spectra at two different time intervals while the gas puff is being established in NSTX show very similar characteristics, with the possible exception of a higher contribution of high frequency noise in the trace corresponding to the low flow rate. Third, no significant change in the fluctuation was seen by a Langmuir probe in Alcator C-Mod that was located at the same minor radius as the GPI cloud with and without the gas puff present. It should be pointed out that although the probe was at the same flux surface as the gas cloud, the probe was not necessarily on the same magnetic field line. The physical explanation for these results which indicate an absence of perturbation at the puff levels used in the experiments may be based in the fact that the turbulent structures are elongated along the magnetic field with at least several meters of length. Consequently, they posses a substantial reservoir of energy and particle ''sink'' to quickly accommodate, i.e., parallel transport along field lines, any extra requirements for energy (ionization and/or radiation) or parallel convection of the ionized puff gas particles. The parallel energy loss or particle gain within the turbulent structure can also be balanced almost completely by radial transport between the core and the elongated structure. A radiative energy loss of ~1 kW within the gas cloud is negligible with respect to the power flow into that volume.

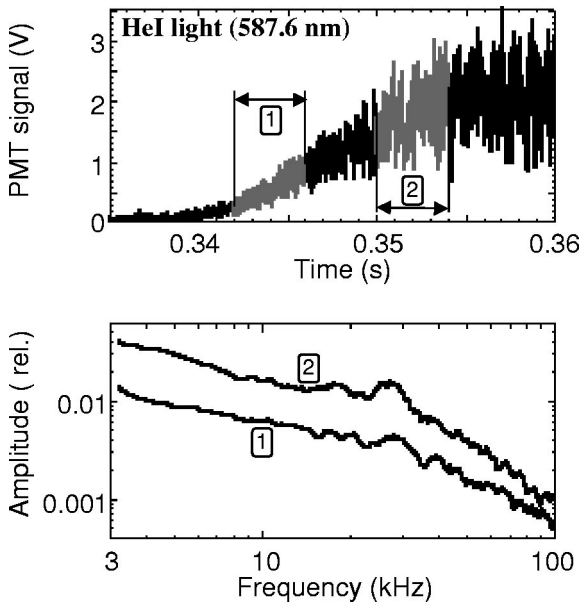

FIG. 2. Similar frequency spectra are seen in NSTX as the helium gas puff is established, giving support to the assumption that the puff does not affect nor produce fluctuations. Top trace is the raw signal from a discrete fast chord looking at a 2 cm ''spot'' on the emitting gas cloud (shot 109036). The bottom traces correspond to the frequency spectra at a low flow rate (1) and a high flow rate (2).

The DEGAS 2 Monte Carlo neutral transport code[15] has been used together with a collisional-radiative model to study the dependence of the line emission on the electron density and temperature and to evaluate the sensitivity of the line emission to variations in these to plasma parameters. In addition, the DEGAS 2 code considers in the case of a deuterium as puff not only the atomic physics for the neutral

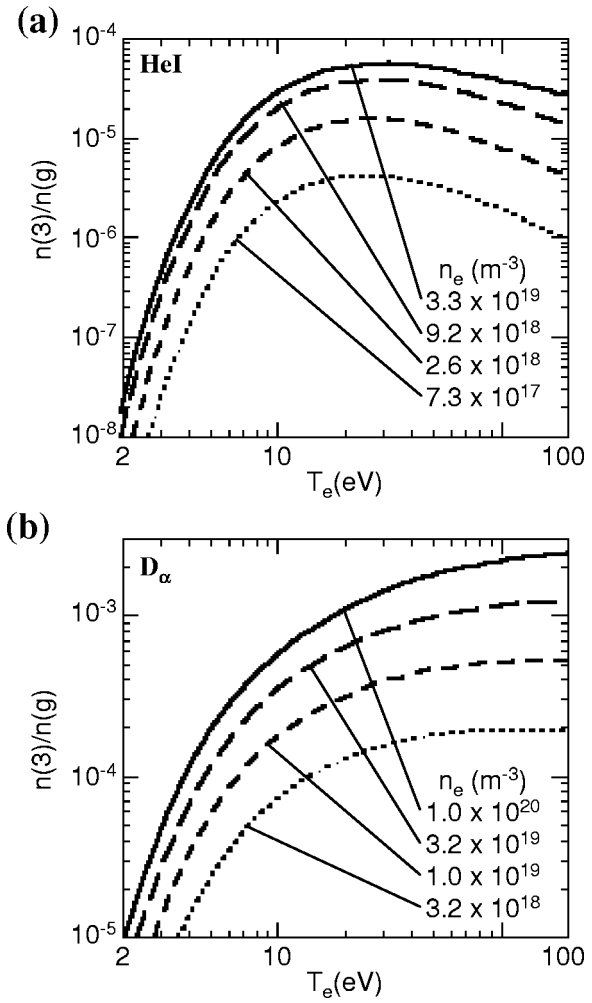

FIG. 3. Dependence of the line emission rates on the electron temperature (T_e) and electron density (n_e) for (a) HeI line at 587.6 nm (b) D_α line at 656.2 nm. The ordinates represent the ratio of the densities between the upper state of the line transition to the ground state. Fluctuations in the line emission can result from either fluctuations on T_e or n_e.

deuterium atoms but the emission from the dissociating D_2 molecule if excited during the collision. (Further details regarding the simulation of D_2 injection into Alcator C-Mod plasmas can be seen in Ref. 16.) Figure 3 shows the dependence of the HeI emission at 587.6 nm (NSTX) and of the D_α emission (Alcator C-Mod) as a function of the electron temperature and parameterized for four different electron densities. The ordinate in both these graphs represents the ratio of the densities between the upper state of the transition to the ground state [i.e., the function $f(n_e, T_e)$ of Eq. (1)]. As can be seen in this figure, fluctuations in the line emission of HeI or D_α can result from either density or temperature fluctuations (or both). Furthermore, the sensitivity on the electron density and temperature varies through the scrape-off layer and the edge. The actual dependence of this sensitivity change depends on the actual electron profiles but in general as one moves radially inward through the scrape-off layer and into the core, finding increasing the electron densities and temperatures, the line emission becomes less sensitive to both the electron density and temperature. Near the peak of light emission in NSTX the local emissivity of HeI at 587.6 nm varies as $S \propto n_e^{0.7} T_e^{0.5}$, whereas near the peak of the D_α emission (Alcator C-Mod) the local emissivity varies as $S \propto n_e^{0.6} T_e^{0.5}$.

Despite this complicated relationship, DEGAS 2 simulations have shown that the spatial structures imposed as perturbations on n_e and/or T_e can be observed in the corresponding line emission. As a consequence of this, analysis of the emission should yield similar wave number spectra than those in the subjacent electron fluctuations either if the density or temperature have dominant fluctuations or if the fluctuations in these to parameters are in phase. Another result from DEGAS 2 simulations for the case of deuterium is that ''shadowing,'' that is, the depletion of the neutral gas flow due to a localized higher ionization rate upstream of the flow, although present is not a significant effect if only emission from atoms is considered.[16] In this case the emission downstream can be affected by a ~20% at most for a 50% modulation in the electron density respect to the time-averaged profiles. Nevertheless, the inclusion of line emission from excited deuterium atoms while still in molecular state, due to its strong dependence on the electron temperature, increases the shadowing effect to over 50%. Shadowing studies have not yet been performed for helium puffs but it is expected that the results will be similar to the deuterium case without molecular effects, i.e., shadowing not significant.

Simulations with DEGAS 2 have resulted in the basic understanding between the relationships between the line emission and the electron density and temperature described above. Work with these simulations continues to incorporate several aspects that may be relevant to the interpretation of GPI diagnostic data. DEGAS 2 currently assumes toroidal symmetry while the real GPI gas puffs are localized toroidally. The 3D geometry needs to be incorporated into the code and their effect on the emission analyzed. In a similar way, metastable helium states are not currently included, which may affect the HeI emission. Finally, DEGAS 2 should be applied to results from edge turbulence simulation in a time-dependent manner. In this way the line emission at each instant in time of the turbulence simulation can be calculated from the perturbed electron density and temperature 2D profiles, including shadowing effects. The time evolving 2D line emission profiles can then be projected into ''images'' similar to those produced in the experiment by means of the GPI diagnostic. The simulated images will then naturally contain the loss-of-resolution effects described above and the reduced data from these images (frequency spectra, spatial *k*-number spectra correlation analysis, turbulent flow analysis, etc.) can be compared to those obtained from the GPI diagnostic and their associated discrete fast chords.

III. RESULTS

In this section we present some typical results from both NSTX and Alcator C-Mod. These results do not intend to be complete nor to give a full description of the physical phenomena involved since this would be beyond the scope of the current paper but to illustrate the physics issues that can be studied with the help of GPI.

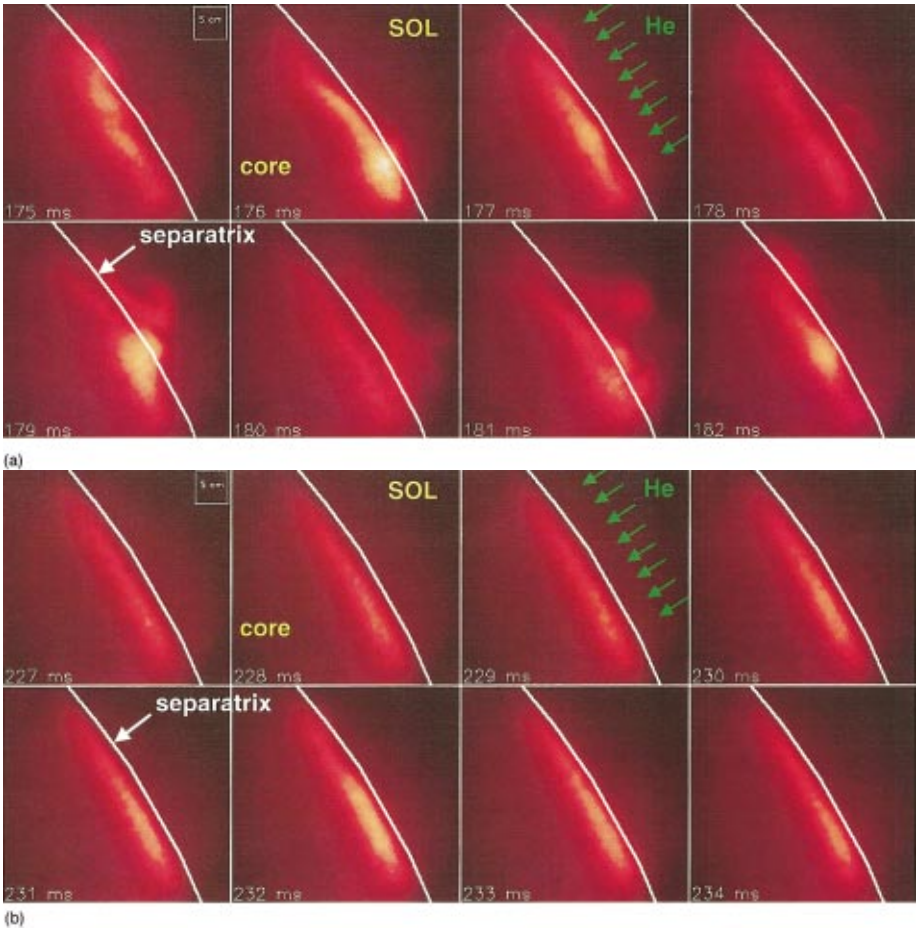

FIG. 4. (Color) Sequences of uncorrelated 10 μs snapshots of HeI emission (587.6 nm) from a gas puff in NSTX. The sequences corresponds to two discharges with 0.9 MA of plasma current and 0.35 T of toroidal field. While the sequence in (a) was obtained during low confinement regime (L-mode, shot 108321), the sequence in (b) corresponds to high confinement regime (H-mode, shot 108316). The line emission from the H-mode discharge appears narrower and smoother than that of the L-mode discharge. The separatrix location is indicated with a white line, the core is located to the bottom left and the scrape-off layer is to the top right.

Snapshots of the gas puff emission from the edge of NSTX are shown in Fig. 4 corresponding to two discharges with 0.9 MA of plasma current and 0.35 T of toroidal field. These snapshots were obtained with the Phantom v.4 digital camera running at 1000 frames/s and with 10 μs exposure of each frame. In the discharge in Fig. 4(a) the plasma has not yet accessed the high confinement regime or H-mode, while in the discharge in Fig. 4(b) the snapshots shown were obtained while the plasma was in H-mode. The time interval between frames (1 ms) in these two sequences is much longer than the autocorrelation time of the turbulence and hence the images for each shot constitute snapshots of the turbulence with no correlation between one frame and the next one. Clear differences can be observed between these two discharges which are characteristic for low confinement regime (L-mode) and H-mode discharges: the line emission from the H-mode discharges: the line emission from the H-mode discharge appears narrower and smoother than that of the L-mode discharge. The narrow emission region observed in H-mode discharges is mainly due to narrower time-averaged edge plasma profiles as simulated using DEGAS 2 using the time-averaged electron density and temperature profiles. While it is observed that L-mode discharges have characteristically intermittent features (or ''blobs'') in the scrape-off layer, the incidence of blobs in H-mode discharges is much smaller with blobless images being more prevalent than those where blobs can be seen. The intermittent fluctuations in the scrape-off layer represent a 100% modulation, while the more Gaussian fluctuations seen at the edge have typically a $\sim$20% modulation respect to the average value.

Using the PSI-3 (or PSI-4) camera and taking the 12 (28) successive frames at a high frame rate ($\geqslant$100 kHz), the dynamics of the turbulence can be followed for a short period of time. In these movies the turbulent features often appear to be born near the separatrix and propagate predominantly outward and poloidally. Six sequential images showing examples of this in Alcator C-Mod can be seen in Fig. 5. The larger ($\sim$1 cm) features move about 1 diam in an autocorrelation time ($\sim$20 μs), at speeds up to $\sim$0.5 m/ms. In some cases, they appear as eddies, turning over once in a lifetime. In other cases ''coherent,'' propagated wavelike patterns are seen, qualitatively similar to some of the NSTX observations. (A more complete analysis of GPI data from Alcator C-Mod can be seen in Ref. 8.)

In contrast to the clear differences in the NSTX images taken during the L- and H-mode confinement phases, in

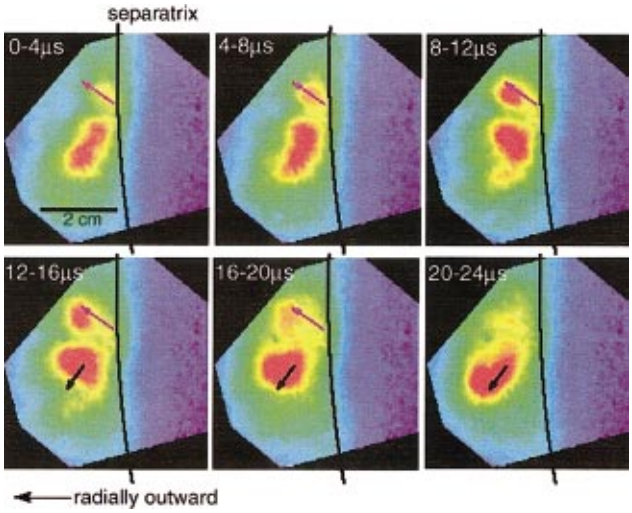

FIG. 5. (Color) Six successive frames of a 250 kHz movie showing the space and time evolution of the edge turbulence in Alcator C-Mod (shot 1010726015). The black line shows the separatrix. The arrows show movement of two ''blobs,'' one moving outward (toward the vessel wall) and upward, the other moving outward and down. Both arrows remain in the same position frame-to-frame.

C-Mod no obvious differences in the spatial structure of the scrape-off turbulence between L- and H-mode are observed. It is hypothesized that this is a result of a difference in the emission location in the two devices. On C-Mod the higher edge densities (in both L- and H-mode) result in almost all of the emission coming from the scrape-off layer and very little emission coming from the transport barrier region ~1 cm inside the separatrix. On NSTX the lower scrape-off density during H-mode allows neutral penetration to the barrier region, and thus the reduced turbulence in the barrier region is observed in the NSTX images. It is still interesting to note that the C-Mod result implies that at least the spatial structure of the turbulence in the scrape-off layer is unchanged by the existence of the edge barrier.

IV. CONCLUSIONS

Gas puff imaging, through the 2D imaging of the edge, allows both the poloidal and radial structure to be measured at one instant in time without the need for this structure to be inferred from statistical correlations. The number of pixels in the images is substantially larger than that previously achieved with Langmuir probes[4] or beam emission spectroscopy (BES).[5] The ultrafast framing digital cameras currently available can follow the motion of the turbulent structure for a few autocorrelation times. A new camera is being developed at Princeton Scientific Instruments, the PSI-5, that will be capable of capturing 300 frames with a 64 pixel×64 pixel format at speeds of up to 1 000 000 frames/s increasing the recording time by an order of magnitude respect to the currently available cameras.

Measurements on NSTX and Alcator C-Mod are generally consistent with previous Langmuir probe, reflectometer, and BES measurements. Nevertheless some measurements can only be obtained through GPI. Among these measurements is the complex movement of the 2D edge structure. This movement shows velocity patterns that indicate complex flows at the edge, which may be related to zonal flows. On the other hand, GPI suffers the limitation that it is constrained to the narrow region where the selected line emission is present. In its current incarnation it is limited to the edge and scrape-off layer in the vicinity of the separatrix. This limitation does not apply to BES, although it very much applies to Langmuir probes although for different reasons, i.e., probe survival. In comparison to BES, GPI is simpler.

Finally, gas puff imaging can became a very important tool to benchmark the constantly developing 3D nonlinear electromagnetic codes used for edge turbulence simulations. Among these 3D nonlinear turbulence codes are the DBM code of Hallastschek[17] and Rogers[18] and BOUT code of LLNL.[19] Initial comparisons with these simulations are certainly encouraging.[8,20] These and/or other 3D nonlinear electromagnetic codes are essential in the understanding of the physical processes leading to the edge turbulence, its evolution, and its eventual control.

ACKNOWLEDGMENTS

This work was supported by the U.S. DOE Contract Nos. W-7405-ENG-36, DE-AC02-CHO3073, and DE-FC02-99ER54512.

[1] J. L. Terry, R. Maqueda, C. S. Pitcher, S. J. Zweben, B. LaBombard, E. S. Marmar, A. Y. Pigarov, and G. Wurden, J. Nucl. Mater. **290-293**, 757 (2001).
[2] R. J. Maqueda, G. A. Wurden, S. Zweben, L. Roquemore, H. Kugel, D. Johnson, S. Kaye, S. Sabbagh, and R. Maingi, Rev. Sci. Instrum. **72**, 931 (2001).
[3] M. Endler, H. Neidermeyer, L. Giannone, E. Holzhauer, A. Rudyj, G. Theimer, and N. Tsois, Nucl. Fusion **35**, 1307 (1995).
[4] S. J. Zweben and R. W. Gould, Nucl. Fusion **25**, 171 (1985).
[5] G. R. McKee, R. Ashley, R. Durst, R. Fonck, J. Jakubowski, K. Tritz, K. Burrell, C. Greenfield, and J. Robinson, Rev. Sci. Instrum. **70**, 913 (1999).
[6] S. J. Zweben and S. S. Medley, Phys. Fluids B **1**, 2058 (1989).
[7] R. Maqueda and G. Wurden, Nucl. Fusion **39**, 629 (1999).
[8] S. J. Zweben *et al.*, Phys. Plasmas **9**, 1981 (2002).
[9] M. Endler, J. Nucl. Mater. **266-269**, 84 (1999).
[10] A. J. Wootton, B. A. Carreras, H. Matsumoto, K. McGuire, W. A. Peebles, C. P. Ritz, P. W. Terry, and S. J. Zweben, Phys. Fluids B **2**, 2879 (1990).
[11] S. M. Kaye *et al.*, Phys. Plasmas **8**, 1977 (2001).
[12] I. H. Hutchinson *et al.*, Phys. Plasmas **1**, 1511 (1994).
[13] H. Thomsen, M. Endler, J. Bleuel, A. V. Chankin, S. K. Erents, and G. F. Matthews, Phys. Plasmas **9**, 1233 (2002).
[14] T. Auguste, M. Bougeard, E. Caprin, P. D'Oliveira, and P. Monot, Rev. Sci. Instrum. **70**, 2349 (1999).
[15] D. P. Stotler and C. F. F. Karney, Contrib. Plasma Phys. **34**, 392 (1994).
[16] D. P. Stotler, *et al.*, in Proceedings of the 15th International Conference on Plasma–Surface Interactions in Controlled Fusion Devices, Nagaragawa, Japan, 2002.
[17] K. Hallatsckek and A. Zeiler, Phys. Plasmas **7**, 2554 (2000).
[18] B. N. Rogers, J. F. Drake, and A. Zeiler, Phys. Rev. Lett. **81**, 4396 (1998).
[19] X. Q. Xu and R. H. Cohen, Contrib. Plasma Phys. **38**, 158 (1998).
[20] X. Q. Xu, W. M. Nevins, R. H. Cohen, J. R. Myra, and P. B. Snyder, New J. Phys. **4**, 53 (2002).